Hopping Conduction Observed in Thermal Admittance Spectroscopy

U. Reislöhner, H. Metzner, and C. Ronning
Friedrich-Schiller-Universität Jena, Physikalisch-Astronomische Fakultät, Institut für Festkörperphysik, Max-Wien-Platz 1, D-07743 Jena, Germany
(Received 19 March 2010; published 2 June 2010)

We observe variable-range hopping conduction in thermal admittance spectroscopy and develop a method to evaluate the signal under this condition. As a relevant example of demonstration we employ $Cu(In,Ga)(Se,S)_2$ thin-film solar cells and show that the fundamental $N1$ signal, which has been discussed for more than a decade in terms of minority carrier traps, does not display trap parameters, but is generated by the freezing-out of carrier mobility with decreasing temperature when hopping conduction prevails. This effect offers a new approach to carrier hopping and to semiconductors suffering from small mobility.

DOI: 10.1103/PhysRevLett.104.226403 PACS numbers: 71.55.−i, 61.72.Bb, 72.20.Ee, 84.37.+q

Owing to the enormous relevance of $Cu(In,Ga)(Se,S)_2$ (abbreviated as CIGS) based thin-film solar cells in the field of low-cost and high-efficiency power conversion from renewable energy sources, substantial theoretical work has been done to understand illumination induced effects and efficiency limiting issues [1–4]. Recently Lany and Zunger [4] suggested intrinsic DX centers in CIGS to be responsible for limitations in improving solar cell efficiency through larger absorber band gaps by an increased Ga content. DX centers are strongly localized electronic states within the band gap and are caused by a strong relaxation off the lattice site. In contrast to II–VI and III–V semiconductors, no extrinsic impurities are required in the CIGS system, as calculated by Lany and Zunger [3,4]. The selective suppression of these defects by adapted processing presupposes, however, an appropriate monitoring method. Lately, the Lany-Zunger model has been related by Igalson *et al.* [5] to the most prominent signal observed by thermal admittance spectroscopy (TAS) on CIGS, the so called $N1$ defect, which is discussed in literature for more than a decade in terms of minority carrier traps (e.g., see Refs. [5,6]). TAS is a widespread method to characterize shallow doping and deep traps in semiconductors and is based on the capacitance of the space charge region in *p-n* junctions or Schottky contacts [7]. Thus, measurements at fully processed devices are possible, without the need of additional sample treatments. However, in the case of CIGS evidence of hopping conduction below 200 K [8] and below 160 K [9] was reported. Although the range of hopping conduction coincides with the temperature interval of the TAS measurements, it has not yet been considered in the evaluation. In this Letter, we explore the consequence of carrier hopping on the capacitance measurement process, develop a method to evaluate the signal under this condition, and prove that the theoretically predicted intrinsic DX centers in CIGS [3,4] cannot experimentally be observed by capacitance methods like TAS when hopping conduction prevails.

The capacitance of the device consists of the capacitance of the space charge region which may be superimposed by a trap related capacitance C_t that depends on temperature and frequency of the applied ac voltage (with frequency ω and amplitude V_{ac}) due to carrier trapping and detrapping. When the temperature becomes too small, capture and emission can no longer take place in the experimentally imposed time window and a steplike decrease in $C_t(\omega,T) \propto {e_p}^2/({e_p}^2+\omega^2)$ occurs while the conductance $G(\omega,T)/\omega \propto e_p\omega/({e_p}^2+\omega^2)$ shows a peak [7] when the capture and hole emission rate e_p are equal and $\omega \approx 2e_p$. The emission rate is connected with the trap's activation energy E_A by $e_p \propto T^2 \exp(-E_A/\mathrm{kT})$. Thus, in standard TAS evaluation $\ln(\frac{1}{2}\omega T^{-2})$ is plotted over $1/T$ to reveal E_A. Beside such trap response, the so called carrier freeze-out signal as described by Pautrat *et al.* [10] may appear at sufficiently low temperatures when the final freeze-out condition $\omega\mathrm{CR}=1$ is met. In the latter case, the time constant of the RC device, consisting of the capacitance C of the space charge region and the series resistance R, equals $1/\omega$.

However, in the standard evaluation of TAS spectra, only a dependence of the measured emission rate $e_p = 1/\tau_e$ on trap properties is assumed. This assumption presupposes a sufficiently fast diffusion of carriers prior to the capture process and a very fast drift of emitted carriers out of the space charge region. When the transport times can no longer be neglected, the measured emission rate is $e_p = 1/\tau$ with $\tau = \tau_{\mathrm{diff}} + \tau_e + \tau_{\mathrm{drift}}$. The characteristic times τ_{drift} and τ_{diff} are determined by the mobility μ which is connected with the diffusion constant D in the Einstein relation $D = \mu\mathrm{kT}/e$, where k denotes the Boltzmann factor, T the temperature, and e the elementary charge. For an estimation of the characteristic drift time, τ_{drift}, during the half cycle of the ac signal in reverse bias direction, we assume a constant mean electric field $E = V/L$, with a voltage V and the mean drift length L. This results in a constant drift velocity $v_D = \mu E$ and $\tau_{\mathrm{drift}} \approx L/\mu E (= L^2/\mu EL = L^2/\mu\mathrm{V})$. During the following half cycle in forward bias direction, carriers diffuse back with the diffusion constant D. Proceeding from the Einstein relation and the diffusion length $L = (D\tau_{\text{diff}})^{1/2}$ we get $\tau_{\text{diff}} \approx L^2/D = L^2 e/\mu kT$ and therefore $\tau_{\text{diff}} \gg \tau_{\text{drift}}$ for $kT/e \ll V$, which is usually the case. Baranovskii *et al.* [11] have shown the classical Einstein relation not to be valid exactly when hopping dominates electrical conduction. Then, D/μ becomes a constant independent of temperature and we do not need to distinguish between drift and diffusion and set the characteristic carrier travel time $\tau^* = \tau_{\text{diff}} + \tau_{\text{drift}} \propto 1/D$. When hopping conduction emerges, the diffusivity of the majority carriers decreases strongly with decreasing temperature and the carriers can follow the ac-signal without phase shift only up to a limiting frequency of $\omega_{\max} \approx 1/\tau^* \propto D$. By further lowering the temperature the measured capacitance gets reduced and a step in $C(T)$ appears (corresponding to a peak in G) as a function of frequency, even when the condition $\omega CR < 1$ is fulfilled. This mobility freeze-out effect is a third, hitherto not recognized source for a TAS-signal beside trap response and carrier freeze-out. Faster carrier emission processes which may take place cannot be observed under this condition and the measured apparent emission rate e_p is approximately given by $1/\tau^*$ and thus $e_p \propto D$.

We investigated highly efficient $Cu(In,Ga)(Se,S)_2$ cells (efficiency around 14%, produced in the AVANCIS R&D pilot line [12]) which are based on a p-n junction between a thin n-type In_2S_3 buffer layer (thickness about 50 nm) and a thick p-type $Cu(In,Ga)(Se,S)_2$ layer with a thickness of about 1.5 μm. Details are described by Palm *et al.* [13]. The thin buffer layer is assumed to be completely depleted and according to our C-V profiling (not shown here), the space charge region extends from 0.5 μm at $V = 0$ V to 1 μm at $V = -1$ V ($\varepsilon = 12$) mainly in the CIGS layer, and shows an acceptor concentration increasing with depth from 2 to 4×10^{15} cm^{-3} independent of temperature between 50 and 200 K. The CV measurements were performed with adjusted frequencies of 1 kHz and below to prevent the mobility related problems, which are discussed in the following. From the known relation for the conductivity $\sigma = \mu pe$, we obtain the carrier mobility by setting $\mu = d/peR_A$, where d is the distance between the end of the space charge region and the back contact, which is estimated to be roughly 1 μm. R_A is the product of series resistance and area, and p denotes the free hole concentration. Because of the increasing acceptor concentration with depth, we assume a mean hole concentration of $p = 5 \times 10^{15}$ cm^{-3} to be relevant in the neutral zone.

We deduced the series resistance of the device by IV measurements in the dark at a high forward bias of 1 V to minimize blocking effects from a small conduction band offset [14] between buffer and CIGS absorber. The series resistance, which is essentially determined by the thick CIGS layer, increases strongly with decreasing temperature: $R_A(200\text{ K}) = 2.4\ \Omega\,\text{cm}^2$, $R_A(150\text{ K}) > 12\ \Omega\,\text{cm}^2$, $R_A(100\text{ K}) > 160\ \Omega\,\text{cm}^2$, $R_A(75\text{ K}) > 1\text{ k}\Omega\,\text{cm}^2$, $R_A(50\text{ K}) > 11\text{ k}\Omega\,\text{cm}^2$. Furthermore, the resistance becomes increasingly voltage dependent below 200 K and decreases with increasing forward bias. Since CIGS is known to be heavily compensated [15], we expect a decreasing resistance when the mean concentration of ionized compensating donors is reduced due to higher minority carrier injection under increasing forward bias. Hence, the resistance values deduced above at 1 V give only a lower limit because TAS measurements are not performed at forward bias. Therefore, the corresponding mobility values drop to less than 10^{-2} cm^2/V s at 150 K and even 10^{-5} cm^2/V s at 50 K.

However, large mobilities of 3–22 cm^2/V s between 200 and 125 K were reported in $Cu(In,Ga)Se_2$ by Lee *et al.* [16] and Ćwil *et al.* [17], who obtained the carrier concentration by CV profiling and the specific resistance ρ from the dielectric relaxation time $\omega^{-1} \approx \rho\varepsilon$, with the dielectric constant ε, using high-frequency admittance measurements [18]. Unfortunately, the conductivity is enhanced by an ac component σ_ω when hopping conduction prevails [19–21]. In this case, the deduced mobility gets greatly overestimated by setting $\sigma_{\text{dc}} = \sigma_{\text{tot}}$. The ac conductivity under hopping conduction is known to obey a power law $\sigma_\omega = A\omega^s$, where A is a constant, depending on temperature and degree of compensation, and the exponent s denotes a number slightly smaller than 1 [19]. Time resolved measurements of the photocurrent by Dinca *et al.* [22] reveal hole drift mobilities between 0.02 and 0.7 cm^2/V s in the range of 100–300 K but without a distinct temperature dependence. However, these measurements probe the drift mobility in the depleted zone near the interface [22], while we determined the mobility in the neutral region which is relevant for the present work. A strongly decreasing mobility in $CuGaSe_2$ with decreasing temperature down to about 0.4 cm^2/V s at 100 K and the onset of hopping conduction below 160 K is reported by Siebentritt [9] using Hall-effect but assuming band transport for the evaluation. However, even the determination of the Hall sign in the case of hopping motion needs detailed knowledge of geometrical arrangements of hopping sites, as well as the nature (s- or p-like) and the orientation of the involved orbitals [23]. The absolute value of the mobility is therefore not in contradiction to our results.

Thus, we adopt the conclusion of variable-range hopping (VRH) [8] connected with the small mobility values we deduced and estimate the corresponding limiting frequencies to compare it with the frequency interval 10^2–10^6 Hz, which is typically used in TAS measurements. Since this interval spans 4 orders of magnitude, we use the classical Einstein relation to simplify matters. The associated error of D/μ is less than a factor of 5 even at 50 K, as demonstrated by Baranovskii *et al.* [11]. With $V = 1$ V, which is in the order of the built-in voltage, and $V_{\text{ac}} = 50$ mV a typical change of depletion depth during one ac cycle is about $L = 0.05$ μm (which equals the

Debye length) one obtains as limiting frequencies $f_{\max}(150\ \mathrm{K}) < 900\ \mathrm{kHz}$, $f_{\max}(100\ \mathrm{K}) < 40\ \mathrm{kHz}$ and $f_{\max}(50\ \mathrm{K}) < 300\ \mathrm{Hz}$. These frequencies and the corresponding temperature interval coincide with typical TAS results on CIGS-cells as shown in Fig. 1. The measurements were performed in the dark at 0 V bias and $V_{\mathrm{ac}} = 50$ mV. The standard evaluation of the large conductance peaks between 55 and 200 K yield a curved Arrhenius-plot [Fig. 2(a)]. This nonlinear behavior is typical for the $N1$ signal and was ascribed to thermally assisted tunneling effects [24]. By evaluating the slope, regardless of the nonlinear behavior, we get activation energies between 29 and 50 meV. The small peaks at the low temperature side below 55 K [inset of Fig. 1(a)] appear to originate from carrier freeze-out, because the geometric layer thickness of about 1.5 μm corresponds to a capacitance of 7 $\mathrm{nF\,cm^{-2}}$ (assuming $\varepsilon = 12$) which is approximately measured at the lowest temperature. However, the carrier freeze-out condition is not met because $\omega \mathrm{CR}_A$ exceeds unity by more than 2 orders of magnitude. Disregarding this, the standard evaluation in terms of carrier freeze-out as described above [10] reveals an apparent activation energy of $E_A = 47$ meV (not shown here).

We now apply the appropriate evaluation as presented above by setting $\omega = 1/\tau \propto D$. In other words, we observe the time constant of hopping carriers in answer to the applied ac voltage, similar to the time constant of trapping and detrapping of carriers at traps within the space charge region in normal TAS. To calculate the temperature dependence of D in the case of VRH-conduction we follow the approach of Paasch *et al.* [25] setting $D = H^2 W$, where H denotes the hopping distance and W the probability for a hopping process. The derivation of Mott's law [26] for variable-range hopping yields $H \propto T^{-1/4}$ and the famous proportionality $W \propto \exp(-B/T^{1/4})$, with the constant $B = (16\alpha^3/kN_{E_F})^{1/4}$ which is determined by the density of states N_{E_F} (per unit energy) around the Fermi energy [8] and the decay length $1/\alpha$ of the localized wave function [26]. Thus, we replace the usual Arrhenius evaluation $\ln(\frac{1}{2}\omega T^{-2})$ vs T^{-1} by plotting $\ln(\omega T^{1/2})$ vs $T^{-1/4}$ and the result is a straight line as shown in Fig. 2(b). From the slope $B = 95 \pm 2\ \mathrm{K}^{1/4}$ and assuming $1/\alpha = 1$ nm (following Schmitt *et al.* [8]) we get the density of states $N_{E_F} = 2.3 \times 10^{18}\ \mathrm{eV^{-1}\,cm^{-3}}$ in perfect agreement with Schmitt *et al.* who obtained $N_{E_F} = 2.4 \times 10^{18}\ \mathrm{eV^{-1}\,cm^{-3}}$ by dc-conduction measurements on CIGS films.

Depending on how far the mobility freeze-out has diminished the measured capacitance a more or less pronounced final step in $C(T)$ or peak in $G(T)$, respectively, may eventually appear at low temperature when the final freeze-out condition $\omega\mathrm{CR} = 1$ is met. This may be caused by ongoing mobility freeze-out or carrier freeze-out. In the present case, the carrier concentration remains almost constant and carrier freeze-out is ruled out. At the lowest

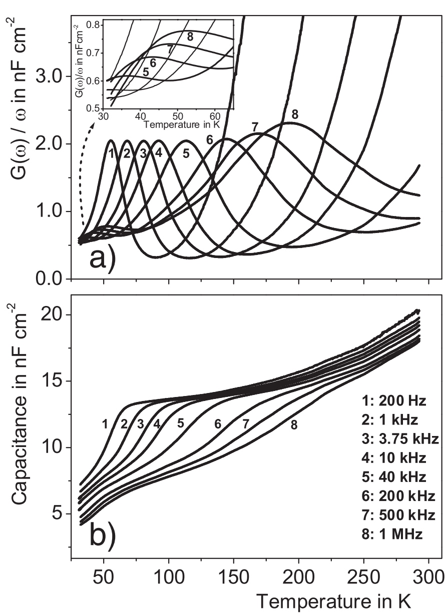

FIG. 1. Conductance (a) and capacitance spectra (b) of a CIGS thin-film solar cell as a function of temperature and frequency. For clarity, only 8 out of 32 measured curves are displayed.

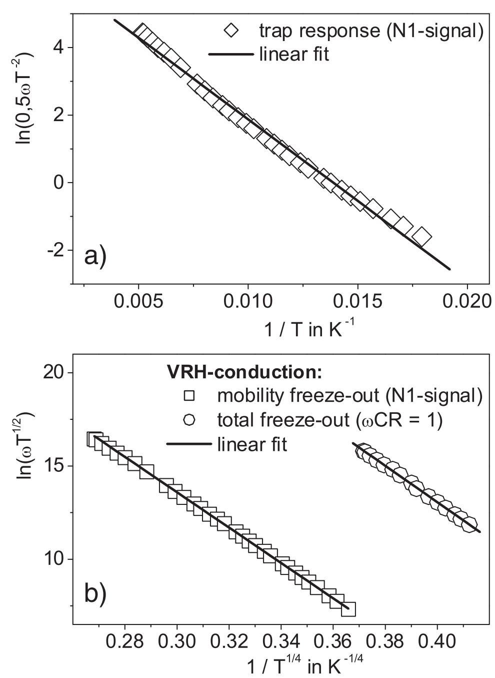

FIG. 2. (a) Standard evaluation of the trap response obtained from Fig. 1(a) gives the known curved line. A linear fit over the complete temperature range gives an activation energy of 42 meV. (b) The evaluation in terms of mobility freeze-out under VRH conduction shows a clear linear behavior. Only $G(\omega)$-maxima below 150 K were used for the linear fit, to avoid the influence of a transition region in the conduction mechanism. The evaluation of total freeze-out ($\omega\mathrm{CR} = 1$) for $G(\omega)$ peaks at $T < 55$ K [see inset if Fig. 1(a)] according to VRH conduction gives a parallel line.

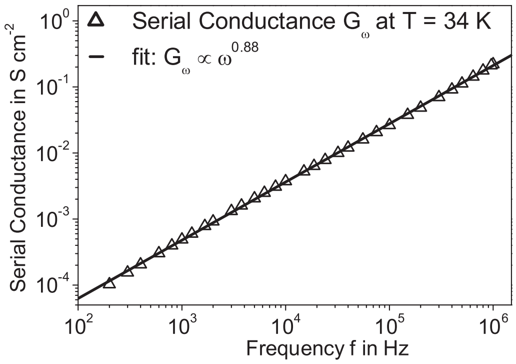

FIG. 3. Measured serial conductance as a function of frequency at $T = 34$ K. The fit confirms a power law $G(\omega) = A\omega^s$ as expected in the case of hopping conduction and yields $G^{-1}(f = 1\text{ MHz}) = 5\ \Omega\,\text{cm}^2$ which is small compared to the dc resistance $R_A > 11\ \text{k}\Omega\,\text{cm}^2$ as deduced from IV measurements.

accessible temperature $T = 34$ K we measure a serial resistance $1/G_\omega = 5\ \Omega\,\text{cm}^2$ at $f = 1$ MHz which is small compared to the dc resistance $R_A(50\text{ K}) > 11\ \text{k}\Omega\,\text{cm}^2$. Because of this strong ac-based enhancement of the total conductivity, the freeze-out condition becomes $\omega\text{CR}_A \gg 1$ when it is expressed only in terms of the dc-resistance $R_{\text{dc}} \equiv R_A$. Therefore, the small low temperature signal in Fig. 1(a) may indeed be interpreted as total freeze-out effect. The evaluation is performed the same way as shown above, because the VRH conductivity is given by $\sigma \propto T^{-1/2}\exp(-B/T^{1/4})$ [25,26] and the condition $\omega\text{CR} = 1$ reveals the same proportionality $\omega \propto 1/R \propto \sigma \propto T^{-1/2}\exp(-B/T^{1/4})$. As demonstrated in Fig. 2(b), the evaluation of the low temperature peaks ($T < 55$ K) in terms of total freeze-out under the condition of VRH-conduction reveals a parallel plot ($B = 98 \pm 3\ \text{K}^{1/4}$) within the experimental errors. The measured serial conductance at $T = 34$ K is plotted in Fig. 3 as a function of frequency. The fit clearly reveals a power law $G_\omega = A\omega^s$ as expected in the case of hopping conduction and the exponent $s = 0.88$ is in agreement with Refs. [8,19]. This finding strongly supports the dominance of hopping conduction connected with the consequences as discussed in this Letter.

In summary, a too small carrier mobility, which is expected in case of hopping conduction, inhibits the observation of carrier trapping and detrapping at traps by thermal admittance spectroscopy. Then, the admittance signal displays the freezing-out of majority carrier mobility instead of trap response. As shown, intricate interpretations concerning the origin of the $N1$ signal in CIGS and the reason for its curved Arrhenius representation become redundant accepting the transition to variable-range hopping conduction at low temperatures and its implications to the TAS measurement process. The here presented evaluation offers a new access to carrier hopping, density of states, and semiconductors suffering from small mobility, even when Hall effect is no longer applicable.

We thank Dr. Palm and Dr. Dalibor of AVANCIS GmbH & Co. KG for interesting discussions and providing the samples.

[1] J. Vidal *et al.*, Phys. Rev. Lett. **104**, 056401 (2010).
[2] S. B. Zhang, S. H. Wei, and A. Zunger, Phys. Rev. Lett. **78**, 4059 (1997).
[3] S. Lany and A. Zunger, J. Appl. Phys. **100**, 113725 (2006).
[4] S. Lany and A. Zunger, Phys. Rev. Lett. **100**, 016401 (2008).
[5] M. Igalson, A. Urbaniak, and M. Edoff, Thin Solid Films **517**, 2153 (2009).
[6] R. Herberholz, M. Igalson, and H. W. Schock, J. Appl. Phys. **83**, 318 (1998).
[7] G. Vincent, D. Bois, and P. Pinard, J. Appl. Phys. **46**, 5173 (1975).
[8] M. Schmitt, U. Rau, and J. Parisi, Phys. Rev. B **61**, 16052 (2000).
[9] S. Siebentritt, Thin Solid Films **480–481**, 312 (2005).
[10] J. L. Pautrat, Solid State Electron. **23**, 1159 (1980).
[11] S. D. Baranovskii, T. Faber, F. Hensel, and P. Thomas, Phys. Status Solidi B **205**, 87 (1998).
[12] AVANCIS GmbH & Co. KG, www/avancis.de.
[13] J. Palm, V. Probst, and F. H. Karg, Solar Energy **77**, 757 (2004).
[14] I. L. Eisgruber *et al.*, Solar Energy Mater. Sol. Cells **53**, 367 (1998).
[15] I. Dirnstorfer *et al.*, Phys. Status Solidi A **168**, 163 (1998).
[16] J. Lee, D. Cohen, and W. N. Shafarman, Thin Solid Films **480–481**, 336 (2005).
[17] M. Ćwil *et al.*, Thin Solid Films **515**, 6229 (2007).
[18] D. V. Lang, J. D. Cohen, and J. P. Harbison, Phys. Rev. B **25**, 5285 (1982).
[19] M. Pollak and T. H. Gebale, Phys. Rev. **122**, 1742 (1961).
[20] K. Jonscher, J. Non-Cryst. Solids **8–10**, 293 (1972).
[21] I. P. Zvyagin, Phys. Status Solidi B **97**, 143 (1980).
[22] S. A. Dinca *et al.*, Phys. Rev. B **80**, 235201 (2009).
[23] D. Emin, Philos. Mag. **35**, 1189 (1977).
[24] P. Zabierowski and M. Igalson, Thin Solid Films **361–362**, 268 (2000).
[25] G. Paasch, T. Lindner, and S. Scheinert, Synth. Met. **132**, 97 (2002).
[26] N. F. Mott and E. A. Davies, *Electronic Processes in Non-Crystalline Materials* (Oxford University Press, London, 1979).